ORBIT MECHANICS ABOUT SMALL ASTEROIDS

D.J. Scheeres

Department of Aerospace Engineering

The University of Michigan

Abstract

Space missions to small solar system bodies must deal with multiple perturbations acting on the spacecraft. These include strong perturbations from the gravity field and solar tide, but for small bodies the most important perturbations may arise from solar radiation pressure (SRP) acting on the spacecraft. Previous research has generally investigated the effect of the gravity field, solar tide, and SRP acting on a spacecraft trajectory about an asteroid in isolation and has not considered their joint effect. In this paper a more general theoretical discussion of the joint effects of these forces is given.

1   Introduction

Space missions to small solar system bodies such as asteroids and comets face significant dynamical challenges. However these bodies are also of great interest to space scientists. Furthermore, small Near Earth Asteroids (NEA) are the most energetically accessible bodies in the solar system, and hence are a natural target for low cost space missions. The special challenges faced by spacecraft missions to these bodies are the relatively strong solar radiation pressure (SRP) forces that act on a spacecraft, the irregular mass distribution that can affect spacecraft in close proximity, and the gravitational effects of the sun, present through direct attraction and through the orbital motion of the asteroid in inertial space. In some mission scenarios, such as that encountered by the Japanese Hayabusa mission to asteroid Itokawa [1], these concerns lead to a mission design that does not have the spacecraft orbit the small body but instead maintains a quasi-stationary position in the asteroid-sun fixed frame enabled by frequent thruster firings. This introduces additional constraints, however, such as the need for frequent control thrusts, and also prevents precision estimation of the physical parameters of the asteroid in some cases. It also limits the lifetime of the orbiter, in that the spacecraft cannot stay indefinitely at the asteroid with no operator intervention. In the current paper we study the orbit mechanics of a spacecraft in orbit about a small body such as an asteroid. The purpose is to outline the limits that exist for stable orbital motion, so a clear determination can be made between when orbiting is feasible and when a spacecraft must instead hover about a small body. Specifically, we study a class of orbits that are stable against SRP perturbations over long time spans, and determine what the effect of the small body mass distribution is on these orbits.

To analyze the stability of the proposed close proximity operations we apply a general analytical methodology that rests on numerous studies of specific asteroids. We assume that the asteroid is modeled as a tri-axial body with 2nd degree and order gravity field coefficients, and incorporate the perturbative force of solar radiation pressure. It has been demonstrated previously that it is the 2nd degree and order gravity field terms that dominate the orbital stability for close proximity motion to uniformly rotating asteroids [2, 3, 4, 5], and that solar radiation pressure can destabilize spacecraft motion about a small body [6, 7, 8, 9]. The effect of both the gravity field and solar radiation pressure perturbations on the orbital evolution of a spacecraft can be characterized with analytical theories of motion. Using these theories we can develop a theory for characterizing whether close proximity operations about a small asteroid model is feasible or not. For characterizing stability against solar radiation pressure we apply the theory developed in [6, 7, 8] given the total mass of the asteroid, the asteroid orbit, and the mass to area ratio of the spacecraft. These provide us specific orbital limits and specific orbit designs to ensure a safe trajectory. For motion close to the body we apply theory developed in [2, 5] for the interaction of orbiters with non-spherical, rotating mass distributions.

Using the results reported here, questions of interaction between the solar radiation pressure and mass distribution perturbations can be taken into account. For a particular asteroid and spacecraft one can derive conditions under which there exists an interval of orbit radii that are robustly stable against both the destabilizing effects of solar radiation pressure (which becomes stronger for larger orbit radii) and interactions with the mass distribution (which becomes stronger for smaller orbit radii). These considerations lead to a nominal orbit design that places the orbit plane parallel to the asteroid terminator plane. This configuration is essentially a frozen orbit for motion about a small asteroid and yields constant orbit elements on average except for the longitude of ascending node, which becomes synchronized with the asteroid's orbital motion about the sun. This synchronicity even persists for a highly eccentric asteroid orbit. When traveling through aphelion, however, the reduced precession rate of the spacecraft orbit can be more easily be perturbed by the precession rate induced by the asteroid mass distribution. This can lead to fluctuation of the orbit eccentricity and can make the orbit unstable. We develop specific bounds on fluctuations in eccentricity and discuss conditions for when this can destablize an orbit.

2 Environment Models

To begin our discussion we provide a brief review of the small body environment and force perturbations. These are split between the asteroid specification and the relevant force perturbations.

2.1 Small Body Model

We assume that the small body is on an elliptic orbit about the sun, and that its motion is well characterized by simple Keplerian dynamics over time spans of interest. This is generally true unless a close passage by a planet occurs, a situation that happens only infrequently. Of specific interest is the varying position vector between the asteroid and the sun, $\mathbf{d} = d\hat{\mathbf{d}}$. Both the magnitude d and a direction $\hat{\mathbf{d}}$ are functions of the asteroid true anomaly ν:

$$d = \frac{P}{1 + E\cos\nu} \tag{1}$$

$$\hat{\mathbf{d}} = \cos\nu\,\hat{\mathbf{x}} + \sin\nu\,\hat{\mathbf{y}} \tag{2}$$

where $\hat{\mathbf{x}}$ is the unit vector pointing to the orbit perihelion, $\hat{\mathbf{y}}$ is the unit vector in the heliocentric plane of motion and normal to $\hat{\mathbf{x}}$. The cross product of these two vectors defines the orbit normal, specified as $\hat{\mathbf{z}}$, about which the asteroid revolves.

Another important specification for the asteroid is its mass distribution and rotation pole. Here we assume the asteroid is uniformly rotating about its maximum moment of inertia. For our detailed analytical discussions we only consider the effect of the $C_{20} = -J_2$ oblateness gravity field coefficient, although the effect of the C_{22} ellipticity gravity field coefficient is discussed in general terms. These gravity field coefficients can be specified by the mass-normalized moments of inertia of the body and equal:

$$C_{20} = -\frac{1}{2}\left(2I_z - I_x - I_y\right) \tag{3}$$

$$C_{22} = \frac{1}{4}\left(I_y - I_x\right) \tag{4}$$

where $I_x \leq I_y \leq I_z$ are the principle moments of inertia of the body.

The asteroid rotation pole is assumed to be fixed in inertial space. For convenience we specify its orientation relative to the above described orbital frame by an obliquity angle β measured between the orbit normal $\hat{\mathbf{z}}$ and asteroid rotation pole $\hat{\mathbf{p}}$, and a right ascension angle α measured between the vector $\hat{\mathbf{z}} \times \hat{\mathbf{p}}$ and $\hat{\mathbf{x}}$. With these definitions the asteroid rotation pole can be explicitly specified as:

$$\hat{\mathbf{p}} = \sin\beta\sin\alpha\,\hat{\mathbf{x}} - \sin\beta\cos\alpha\,\hat{\mathbf{y}} + \cos\beta\,\hat{\mathbf{z}} \tag{5}$$

2.2 Force Models

Next we summarize the relevant force models that act on a small body orbiter. These include solar radiation pressure (SRP), mass distribution effects, and solar gravitational effects.

Solar radiation pressure: We use a minimal model for the SRP acceleration, modeling the spacecraft as a flat plate oriented at the sun. It is possible to generalize this model, however the essential dynamics of motion under this force will not be changed significantly. We start with a force potential formulation of the model:

$$R_g \;=\; g\hat{\mathbf{d}} \cdot \mathbf{r} \tag{6}$$

where g is the acceleration, $\hat{\mathbf{d}}$ is the direction in which it acts (away from the sun) and $\mathbf{r}$ is the position of the spacecraft relative to the asteroid center of mass. The acceleration force is computed as the partial of R_g with respect to $\mathbf{r}$ and is $\mathbf{g} = g\hat{\mathbf{d}}$ and the acceleration magnitude is computed as:

$$g \;=\; \frac{\beta}{d^2} \tag{7}$$

where $\beta = (1+\rho)G_1/B$, $G_1 \sim 1 \times 10^8$ kg-km^3/(s^2-m^2), B is the spacecraft mass to area ratio in kg/m^2, ρ is the reflectance of the spacecraft, $\beta = (1+\rho)G_1/B$, and d is the distance between the sun and small body in km. This model assumes that the spacecraft is modeled as a flat plate facing the sun, and that the absorbed solar radiation is radiated away uniformly. Note the dependence of g on the distance between the asteroid and sun, thus the SRP force varies in time between a maximum at perihelion and a minimum at aphelion.

Mass distribution: The attraction of the small body is initially modeled as a point mass, but we will later consider the effect of a 2nd degree and order gravity field perturbation. Inclusion of the 2nd degree and order field is sufficient to capture the main effects of non-sphericity in the mass distribution. Higher order gravity coefficients can be important, but do not have such a dominant effect on the qualitative dynamics of motion for this system. For our situation where the rotation axis of the body is not aligned with the $\hat{\mathbf{z}}$ axis of the main coordinate frame, it is useful to state this term in vector form.

$$R_2(\mathbf{r}) \;=\; -\frac{\mu}{2r^3}C_{20}\left[1 - 3(\hat{\mathbf{r}} \cdot \hat{\mathbf{p}})^2\right] + \frac{3\mu}{r^3}C_{22}\left[(\hat{\mathbf{r}} \cdot \hat{\mathbf{s}})^2 - (\hat{\mathbf{r}} \cdot \hat{\mathbf{q}})^2\right] \tag{8}$$

where we assume that the unit vectors $\hat{\mathbf{p}}$, $\hat{\mathbf{q}}$, $\hat{\mathbf{s}}$ are aligned with the body's maximum, intermediate, and minimum axes of inertia. For our analytical work we will neglect the C_{22} coefficient, although this has been studied in detail elsewhere [5].

Solar gravitation: Also necessary to incorporate for some analyses is the perturbation of the sun's gravity on the motion of an orbiter. This can be modeled as a 3rd body perturbation, and its functional form can be simplified by performing an appropriate expansion which is essentially Hill's approximation. In this paper we do not deal with the solar gravitation in any substantial way, and we refer the reader to [7] for an in-depth discussion.

3 Equations of Motion

Combining the above force models we can define the equations of motion for a spacecraft in orbit about an asteroid. In an inertially fixed frame centered at the asteroid, they can be stated as:

$$\ddot{\mathbf{r}} \;=\; \frac{\partial U}{\partial \mathbf{r}} \tag{9}$$

$$U(\mathbf{r}) \;=\; \frac{\mu}{r} + R(\mathbf{r}) \tag{10}$$

$$R(\mathbf{r}) \;=\; R_2(\mathbf{r}) + R_g(\mathbf{r}) + R_S(\mathbf{r}) \tag{11}$$

We can equivalently state the problem in terms of the Lagrange Planetary Equations:

$$\frac{da}{dt} \;=\; \frac{2}{na}\frac{\partial R}{\partial \sigma} \tag{12}$$

$$\frac{de}{dt} \;=\; \frac{1-e^2}{na^2 e}\frac{\partial R}{\partial \sigma} - \frac{\sqrt{1-e^2}}{na^2 e}\frac{\partial R}{\partial \omega} \tag{13}$$

$$\frac{di}{dt} = \frac{\cot i}{na^2\sqrt{1-e^2}}\frac{\partial R}{\partial \omega} - \frac{1}{na^2\sqrt{1-e^2}\sin i}\frac{\partial R}{\partial \Omega} \tag{14}$$

$$\frac{d\omega}{dt} = \frac{\sqrt{1-e^2}}{na^2 e}\frac{\partial R}{\partial e} - \frac{\cot i}{na^2\sqrt{1-e^2}}\frac{\partial R}{\partial i} \tag{15}$$

$$\frac{d\Omega}{dt} = \frac{1}{na^2\sqrt{1-e^2}\sin i}\frac{\partial R}{\partial i} \tag{16}$$

$$\frac{d\sigma}{dt} = -\frac{2}{na}\frac{\partial R}{\partial a} - \frac{1-e^2}{na^2 e}\frac{\partial R}{\partial e} \tag{17}$$

where a is the semi-major axis, e is the eccentricity, i is the inclination, ω is the argument of periapsis, Ω is the longitude of the ascending node and $\sigma = -M_o$ where M_o is the mean anomaly at epoch. The additional parameter $n = \sqrt{\mu/a^3}$ is the mean motion.

For each of these equations, there are situations where we wish to pose them in a frame rotating with the sun-line $\hat{\mathbf{d}}$. By definition, this frame rotates at the true anomaly rotation rate, which varies with the distance of the asteroid with the sun. The rotational velocity vector for this rotating frame is $\dot{\nu}\tilde{\mathbf{z}}$ and $\dot{\nu} = \sqrt{\mu_{sun}A(1-E^2)}/d^2$. For example, in a rotating frame the above equations of motion become:

$$\ddot{\mathbf{r}}_r + 2\dot{\nu}\tilde{\mathbf{z}}\cdot\dot{\mathbf{r}}_r + \ddot{\nu}\tilde{\mathbf{z}}\cdot\mathbf{r} + \dot{\nu}^2\tilde{\mathbf{z}}\cdot\tilde{\mathbf{z}}\cdot\mathbf{r} = \frac{\partial U}{\partial \mathbf{r}} \tag{18}$$

where the subscript r denotes a time derivative with respect to the rotating frame, we note that $\ddot{\nu} = -2\mu_{sun}E\sin\nu/d^3$ and that

$$\tilde{\mathbf{z}} = \hat{\mathbf{x}}\hat{\mathbf{y}} - \hat{\mathbf{y}}\hat{\mathbf{x}} \tag{19}$$

using a dyadic notation. The Lagrange Planetary equations are simply modified by subtracting the true anomaly ν from the longitude of the ascending node, $\Omega_r = \Omega - \nu$, yielding the modified equation:

$$\frac{d\Omega_r}{dt} = \frac{1}{na^2\sqrt{1-e^2}\sin i}\frac{\partial R}{\partial i} - \dot{\nu} \tag{20}$$

all else being the same.

4 Orbit Mechanics

The equations of motion stated above can be solved exactly for a number of different special cases. Some of these cases are of interest and can help answer certain fundamental questions such as what is the maximum orbit size before it is stripped away from the central body and what the secular evolution of an orbit subject to SRP. In the following we present some of these exact solutions and their applications. Much of this work has been reported elsewhere, although we bring it together for the first time and add some additional interpretation of these issues.

4.1 Escape conditions

The simplest system to analyze is that of a non-rotating, constant acceleration acting on a spacecraft orbiting about a point mass. This problem is integrable if motion is constrained to a plane containing the acceleration vector, as it is a limiting case of the fixed two-center problem with one of the centers being moved to infinity [10]. This problem was also analyzed extensively by Dankowicz [11, 12, 13, 14] using advanced methods of dynamical systems theory. Dankowicz's analysis considered both the unperturbed problem and various perturbations of it. From the initial analysis of Dankowicz [11] we can extract some very useful results for spacecraft orbit design, which are based on the ideal conservation of the angular momentum about the constant force direction (i.e., the line of action of the solar radiation pressure).

The relevant force potential in this case is $U = \mu/r + g\hat{\mathbf{d}}\cdot\mathbf{r}$ where $\hat{\mathbf{d}}$ is assumed to be stationary with respect to inertial space. The resulting equations of motion are:

$$\ddot{\mathbf{r}} = -\frac{\mu}{r^3}\mathbf{r} + g\hat{\mathbf{d}} \tag{21}$$

We can easily show that the total angular momentum projected onto the $\hat{\mathbf{d}}$ direction is conserved, or $h_d = \hat{\mathbf{d}} \cdot (\mathbf{r} \times \dot{\mathbf{r}})$ is a constant. The form of the equations are simplified if we shift to a cylindrical frame with the axis of the cylinder along $\hat{\mathbf{d}}$ and the radius, ρ, and polar angle, θ, measured perpendicular to this direction. If we assign the $\hat{\mathbf{x}}$ axis to the direction of the acceleration and the $\hat{\mathbf{y}}$ and $\hat{\mathbf{z}}$ axis perpendicular to this we find the simplified set of equations:

$$\ddot{x} = -\frac{\mu x}{r^3} + g \tag{22}$$

$$\ddot{\rho} - \rho\dot{\theta}^2 = -\frac{\mu\rho}{r^3} \tag{23}$$

$$\rho\ddot{\theta} + 2\dot{\rho}\dot{\theta} = 0 \tag{24}$$

where $r^2 = x^2 + \rho^2$. The conserved angular momentum is now $h_d = \rho^2\dot{\theta}$ and can be immediately inferred from integrating Eqn. 24. Eliminating $\dot{\theta}$ through this parameter we find the simplified set of equations and related force potential:

$$\ddot{x} = \frac{\partial U_d}{\partial x} \tag{25}$$

$$\ddot{\rho} = \frac{\partial U_d}{\partial \rho} \tag{26}$$

$$U_d = \frac{\mu}{r} - \frac{1}{2}\frac{h_d^2}{\rho^2} + gx \tag{27}$$

It is important to note that the reduced set of equations still have a Jacobi integral:

$$C = \frac{1}{2}\left(\dot{x}^2 + \dot{\rho}^2\right) - U_d \tag{28}$$

This is directly related to the energy of the system, as if we substitute for $h_d = \rho^2\dot{\theta}$ we find the following:

$$C = \frac{1}{2}\left(\dot{x}^2 + \dot{\rho}^2 + \rho^2\dot{\theta}^2\right) - U \tag{29}$$

where $U = \mu/r + gx$ is the original force perturbation and the velocity term $\dot{x}^2 + \dot{\rho}^2 + \rho^2\dot{\theta}^2 = V_I^2$ where V_I is the magnitude of the total inertial velocity.

These equations have many interesting properties, but the one we focus on is the existence of an equilibrium point that corresponds to a circular orbit, offset from the center of the point mass along the direction $\hat{\mathbf{x}}$ and perpendicular to this same direction. A modified form of this orbit will also play a special role in the more general case accounting for the motion of the asteroid about the sun. The unique aspect of this solution is that it can lose its stability at a certain value of energy, and that this agrees well observed limits for the escape of a spacecraft from an asteroid due to the SRP perturbation.

The equilibrium point is simple to find, solving for $\partial U_d/\partial x = 0$ and $\partial U_d/\partial \rho = 0$:

$$x_{eq} = \frac{g}{\mu}r_{eq}^3 \tag{30}$$

$$\rho_{eq}^4 = \frac{h_d^2}{\mu}r_{eq}^3 \tag{31}$$

where these two equations are still coupled through the relation $r^2 = x^2 + \rho^2$. We note that the crucial parameter is the orbit radius, r, and the ratio g/μ. Once these are specified the value of x and ρ are fixed. We note that by definition $x \leq r$ and thus we find a fundamental limit on the orbit radius, $r \leq \sqrt{\mu/g}$. Conversely, as $\rho \leq r$ as well, we find a lower limit as $h_d^2/\mu \leq r$, which implies a limit $h_d \leq 1/\sqrt{\mu g}$.

To study the stability of this equilibrium point we form the linearized equations of motion and compute the characteristic equation. Evaluation of the system yields a simple condition for stability:

$$x_{eq} \leq \frac{1}{3\sqrt{3}}\sqrt{\frac{\mu}{g}} \tag{32}$$

5

We note that the upper bound on x_{eq} is the value at which the Jacobi integral value takes on its maximum value for all of the relative equilibria, $C_{max} = -2\sqrt{\mu g}/\sqrt{3}$. In [11] the orbit dynamics of the system were studied when the relative equilibrium were unstable, and escape was found to be the common occurrence. From the above analysis we see that when $C < C_{max}$ that there will be two relative equilibrium orbits, one stable with $x < x^*$ and one unstable with $x > x^*$. When $C = C_{max}$ these two equilibrium points coincide at the maximum value of C. This simple relationship allows us to derive a necessary condition for escape of a spacecraft from the asteroid in this simple model, or a sufficient condition for stability. Simply put, if the Jacobi energy of a spacecraft is less than C_{max} and the spacecraft is in the interior region of the zero-velocity surface, then it cannot escape. If its Jacobi energy is equal to or greater than C_{max}, then it is possible for it to escape. In practice we find escape to be the usual situation. Thus, given an initial value of h_d, x and ρ we have a limit for the reduced speed of the system, $(\dot{x}^2 + \dot{\rho}^2)/2 \leq C_{max} + U_d$. We can make this limit simpler and more useful by taking advantage of the special structure of this Jacobi integral, and find a limit on the osculating semi-major axis for stability:

$$a \quad \leq \quad \frac{\sqrt{3}}{4}\sqrt{\frac{\mu}{g}} = a_{max} \tag{33}$$

This serves as a useful design parameter in constraining the maximum orbit size for mission design purposes.

Once the motion of the asteroid about the sun is modeled, by allowing the unit vector $\hat{\mathbf{d}}$ to rotate as a function of time, the conservation of h_d is destroyed and the dynamics of the system become much more complex. Additionally, the solar gravitational effect must be taken into account as it balances the centripetal accelerations that arise from the frame rotation. In [7] this problem is derived and studied in detail. We will only summarize those results here. There are some exact solutions of the system in this case that are stationary in the frame rotating and pulsating with the asteroid-sun distance, and which correspond to periodic orbits in inertial space that follow close to the 2-body motion of the asteroid about the sun. Analysis of these equations provides a necessary condition for a spacecraft to escape which, in the limit of strong SRP perturbation, approaches the limit given above for the non-rotation case. Thus, this provides further validation of the above limit and makes it clear that it is appropriate to use for varying distances between the asteroid and sun.

4.2 Averaged Orbit Mechanics Solutions

Stating the spacecraft motion as a perturbation problem allows us to introduce averaging to the system. This allows one to solve for the general secular motion of an orbiter under SRP, which is found to be quite complex yet integrable, and to identify a set of "frozen orbits" that are suitable for orbiting a spacecraft in. We also present the averaged effect of mass distribution to identify the effect of the asteroid's shape on an orbit.

4.2.1 SRP Perturbation Formulation and Averaging

Given that the perturbation from solar radiation pressure is usually small, it is useful to cast the problem into a perturbation form. The perturbing potential associated with SRP is found in Eqn. 6. We introduce the concept of averaging as this allows us to evaluate the secular effect of the perturbation on our system. The averaged potential is defined as

$$\bar{R}_g \quad = \quad \frac{1}{2\pi}\int_0^{2\pi} R_g dM \tag{34}$$

$$= \quad -\frac{3ag}{2}\mathbf{e}\cdot\hat{\mathbf{d}} \tag{35}$$

where M is the mean anomaly and $\mathbf{e}$ is the eccentricity vector and has magnitude equal to the eccentricity and points towards the orbit periapsis. The average is taken over the unperturbed 2-body motion of the spacecraft about the asteroid, and we hold the direction $\hat{\mathbf{d}}$ fixed initially.

Stated in this form, the rates of change of the orbit elements can be computed by substituting the averaged potential $\bar{R}_g$ into the Lagrange Planetary equations. The simplest observation to make is that

the semi-major axis is conserved on average, and hence the energy of the orbit is conserved on average. The Lagrange Planetary Equations for this case can be integrated in closed form, a fact originally proven by Mignard and Hénon [15], and worked out in detail in [6]. An alternate statement of the perturbation equations is given by [16] and uses the angular momentum and eccentricity vectors as the nominal orbit elements. These are not an immediately obvious choice, as this system is overdetermined in that the 6 components of these two vectors are functions of only 4 orbit elements with secular rates, e, i, ω and Ω. Still, this formulation has a significant advantage in being able to be solved in closed form, a fact originally realized by Richter and Keller [16].

In [16] the standard set of equations for the secular evolution of the eccentricity vector $\mathbf{e}$ and the normalized angular momentum vector $\mathbf{h}$ in the presence of a non-rotating SRP force is found to be:

$$\dot{\mathbf{e}} = \frac{3g}{2}\sqrt{\frac{a}{\mu}}\tilde{\hat{\mathbf{d}}}\cdot\mathbf{h} \tag{36}$$

$$\dot{\mathbf{h}} = \frac{3g}{2}\sqrt{\frac{a}{\mu}}\tilde{\hat{\mathbf{d}}}\cdot\mathbf{e} \tag{37}$$

The normalized angular momentum vector $\mathbf{h} = \sqrt{1-e^2}\hat{\mathbf{h}}$, and thus is normalized by the factor $\sqrt{\mu a}$, which is constant on average.

These equations can be modified to account for the rotation of $\hat{\mathbf{d}}$. Given a frame rotational velocity vector of $\dot{\nu}\hat{\mathbf{z}}$ we find:

$$\dot{\mathbf{e}}_r + \dot{\nu}\tilde{\hat{\mathbf{z}}}\cdot\mathbf{e} = \frac{3g}{2}\sqrt{\frac{a}{\mu}}\tilde{\hat{\mathbf{d}}}\cdot\mathbf{h} \tag{38}$$

$$\dot{\mathbf{h}}_r + \dot{\nu}\tilde{\hat{\mathbf{z}}}\cdot\mathbf{h} = \frac{3g}{2}\sqrt{\frac{a}{\mu}}\tilde{\hat{\mathbf{d}}}\cdot\mathbf{e} \tag{39}$$

where the r subscript indicates time derivative with respect to a rotating frame and will be dropped from this point on. We can write the secular equations as a linear system:

$$\begin{bmatrix} \dot{\mathbf{e}} \\ \dot{\mathbf{h}} \end{bmatrix} = \frac{3g}{2}\sqrt{\frac{a}{\mu}}\begin{bmatrix} -\frac{2\dot{\nu}}{3g}\sqrt{\frac{\mu}{a}}\tilde{\mathbf{z}} & \tilde{\hat{\mathbf{d}}} \\ \tilde{\hat{\mathbf{d}}} & -\frac{2\dot{\nu}}{3g}\sqrt{\frac{\mu}{a}}\tilde{\mathbf{z}} \end{bmatrix}\begin{bmatrix} \mathbf{e} \\ \mathbf{h} \end{bmatrix} \tag{40}$$

While this is a linear differential equation, it is not time-invariant as both $\dot{\nu}$ and g vary in time. It is important to note that the ratio $\dot{\nu}/g$ is time invariant, as both vary inversely with d^2:

$$\frac{2\dot{\nu}}{3g}\sqrt{\frac{\mu}{a}} = \frac{2\sqrt{\mu_{Sun}A(1-E^2)}}{3\beta}\sqrt{\frac{\mu}{a}} \tag{41}$$

This quantity is a constant for a given asteroid, spacecraft and spacecraft orbit, so we define [15]:

$$\tan\Lambda = \frac{3\beta}{2}\sqrt{\frac{a}{\mu\mu_{Sun}A(1-E^2)}} \tag{42}$$

We note that as the SRP perturbation becomes strong, $\Lambda \to \pi/2$, and that as it becomes weak $\Lambda \to 0$.

Despite the time invariance of the ratio, the multiplying factor of the matrix is still time varying. We can eliminate this by changing our independent parameter from time to the true anomaly of the asteroid about the sun, as $\dot{\mathbf{e}} = \frac{d\mathbf{e}}{d\nu}\dot{\nu} = \mathbf{e}'\dot{\nu}$. Then the factor in front of the matrix becomes our newly defined SRP strength parameter, leading to the time-invariant linear differential equations:

$$\begin{bmatrix} \mathbf{e}' \\ \mathbf{h}' \end{bmatrix} = \begin{bmatrix} -\tilde{\mathbf{z}} & \tan\Lambda\tilde{\hat{\mathbf{d}}} \\ \tan\Lambda\tilde{\hat{\mathbf{d}}} & -\tilde{\mathbf{z}} \end{bmatrix}\begin{bmatrix} \mathbf{e} \\ \mathbf{h} \end{bmatrix} \tag{43}$$

where we note that the direction $\hat{\mathbf{d}}$ is now fixed in the rotating coordinate frame. We find it convenient to redefine the independent variable from true anomaly ν to a new angle $\psi = \nu/\cos\Lambda$.

The solution matrix can be reduced to elementary functions, yielding the explicit solution:

$$\begin{bmatrix} \mathbf{e}(\psi) \\ \mathbf{h}(\psi) \end{bmatrix} = \Phi_r(\psi - \psi_o) \begin{bmatrix} \mathbf{e}_o \\ \mathbf{h}_o \end{bmatrix} \tag{44}$$

$$\Phi(\psi) = \cos(\psi)I_{6\times 6} + (1 - \cos(\psi))$$
$$\begin{bmatrix} \cos^2 \Lambda \hat{\mathbf{z}}\hat{\mathbf{z}} + \sin^2 \Lambda \hat{\mathbf{d}}\hat{\mathbf{d}} & -\sin \Lambda \cos \Lambda \left(\hat{\mathbf{z}}\hat{\mathbf{d}} + \hat{\mathbf{d}}\hat{\mathbf{z}} \right) \\ -\sin \Lambda \cos \Lambda \left(\hat{\mathbf{z}}\hat{\mathbf{d}} + \hat{\mathbf{d}}\hat{\mathbf{z}} \right) & \cos^2 \Lambda \hat{\mathbf{z}}\hat{\mathbf{z}} + \sin^2 \Lambda \hat{\mathbf{d}}\hat{\mathbf{d}} \end{bmatrix}$$
$$+ \sin(\psi) \begin{bmatrix} -\cos \Lambda \tilde{\hat{\mathbf{z}}} & \sin \Lambda \tilde{\hat{\mathbf{d}}} \\ \sin \Lambda \tilde{\hat{\mathbf{d}}} & -\cos \Lambda \tilde{\hat{\mathbf{z}}} \end{bmatrix} \tag{45}$$

This combines the explicit solution detailed in [15, 6] in classical orbit elements and the solution in [16] that only provides a solution in the non-rotating case. We note that the solutions are periodic in ψ, repeating every true anomaly $2\pi \cos \Lambda$. Thus, over one heliocentric orbit the solution will advance $1/\cos \Lambda$ times. As the perturbation grows large, and Λ approaches $\pi/2$, the solution will repeat many times. Conversely, as the perturbation grows small the solution will repeat only once every heliocentric orbit. Also, we note that the state transition matrix is ortho-normal and defines a rotation matrix in 6-dimensional space.

We can discuss the existence of frozen orbits for this system. To find them we search for solutions to the algebraic equations:

$$-\tilde{\hat{\mathbf{z}}} \cdot \mathbf{e} + \tan \Lambda \tilde{\hat{\mathbf{d}}} \cdot \mathbf{h} = 0 \tag{46}$$

$$-\tilde{\hat{\mathbf{z}}} \cdot \mathbf{h} + \tan \Lambda \tilde{\hat{\mathbf{d}}} \cdot \mathbf{e} = 0 \tag{47}$$

We note that $\mathbf{e}$ and $\mathbf{h}$ are orthogonal and assume that both are non-zero in magnitude initially. A detailed study of this matrix and its null spaces shows that there are two classes of solutions. First, if we choose $\mathbf{e}$ parallel to $\hat{\mathbf{d}}$ and $\mathbf{h}$ parallel to $\hat{\mathbf{z}}$ the second equation is identically solved and the first equation reduces to a vector equation parallel to the unit vector $\hat{\mathbf{t}}$. It turns out that the direction in which these vectors point is important, thus we introduce the test solutions $\mathbf{e} = e(\hat{\mathbf{d}} \cdot \hat{\mathbf{e}})\hat{\mathbf{d}}$ and $\mathbf{h} = h(\hat{\mathbf{z}} \cdot \hat{\mathbf{h}})\hat{\mathbf{z}}$. Resolving the first equation along the direction $\hat{\mathbf{t}}$ then yields:

$$e(\hat{\mathbf{d}} \cdot \hat{\mathbf{e}}) + \tan \Lambda h(\hat{\mathbf{z}} \cdot \hat{\mathbf{h}}) = 0 \tag{48}$$

We note again that $h = \sqrt{1 - e^2}$, which simplifies the expression to

$$\frac{e}{\sqrt{1 - e^2}} = -(\hat{\mathbf{d}} \cdot \hat{\mathbf{e}})(\hat{\mathbf{z}} \cdot \hat{\mathbf{h}}) \tan \Lambda \tag{49}$$

Thus there are two conditions for a frozen orbit to exist in this configuration:

$$-(\hat{\mathbf{d}} \cdot \hat{\mathbf{e}})(\hat{\mathbf{z}} \cdot \hat{\mathbf{h}}) = 1 \tag{50}$$

$$e = \sin \Lambda \tag{51}$$

This class of frozen orbit were discussed in [6] and called Ecliptic frozen orbits. The orbit lies in the same plane as the asteroid's heliocentric orbit. If the orbit normal is aligned with the heliocentric orbit, periapsis must point towards the sun, otherwise if the orbit normal is anti-parallel to the heliocentric orbit normal, periapsis must point away from the sun. As the perturbation strength grows the orbit approaches rectilinear, while if the perturbation strength vanishes the orbit approaches circular. Due to this, these orbits are not preferred for strongly perturbed situations, as the periapsis has a low altitude. Also, these orbits cross through the asteroid's shadow.

A second frozen orbit solution, called Solar Plane-of-Sky frozen orbits in [6], also exist and are more useful for highly perturbed systems. Now, choose $\mathbf{e}$ parallel to $\hat{\mathbf{z}}$ and $\mathbf{h}$ parallel to $\hat{\mathbf{d}}$ so the Equation 46 is identically solved and Equation 47 reduces to a vector equation again parallel to the unit vector $\hat{\mathbf{t}}$. Again the direction in which these vectors point is important, thus we introduce the test solutions $\mathbf{e} = e(\hat{\mathbf{z}} \cdot \hat{\mathbf{e}})\hat{\mathbf{z}}$ and $\mathbf{h} = h(\hat{\mathbf{d}} \cdot \hat{\mathbf{h}})\hat{\mathbf{d}}$. Resolving Equation 47 along the direction $\hat{\mathbf{t}}$ then yields:

$$e \tan \Lambda (\hat{\mathbf{z}} \cdot \hat{\mathbf{e}}) + h(\hat{\mathbf{d}} \cdot \hat{\mathbf{h}}) = 0 \tag{52}$$

which simplifies again to

$$\frac{e}{\sqrt{1-e^2}} = -(\hat{\mathbf{z}} \cdot \hat{\mathbf{e}})(\hat{\mathbf{d}} \cdot \hat{\mathbf{h}}) \cot \Lambda \tag{53}$$

The two conditions for a frozen orbit to exist in this configuration are:

$$-(\hat{\mathbf{z}} \cdot \hat{\mathbf{e}})(\hat{\mathbf{d}} \cdot \hat{\mathbf{h}}) = 1 \tag{54}$$

$$e = \cos \Lambda \tag{55}$$

The orbit lies in the plane perpendicular to the sun-line, commonly referred to as the terminator plane, a dawn-dusk orbit or a 3o'clock/9o'clock orbit. If the orbit normal points towards the sun, periapsis must point above the orbit plane along the positive $\hat{\mathbf{z}}$ axis, otherwise if the orbit normal points away from the sun, periapsis must point below the orbit plane. As the perturbation strength grows the orbit becomes more circular, while if the perturbation strength vanishes the orbit approaches rectilinear. Due to this, these orbits are preferred for strongly perturbed situations. Also, these orbits avoid the asteroid's shadow. Finally, these orbits are the natural continuation of the equilibrium orbits in the non-rotation case.

4.3 Mass Distribution Perturbation and Averaging

Now we will review the classical result for the averaged effect of a second degree and order gravity field. In order to relate this analysis to the SRP frame requires that the oblateness effect be specified in a general orbit frame, and not one chosen so that the inclination is measured from the symmetry axis. When a general frame for the oblateness perturbation not aligned with the symmetry axis is specified the inclination can also suffer a secular perturbation. To see this we state the oblateness perturbation function in a general vector expression. If the maximum moment of inertia axis of the mass distribution is stipulated as $\hat{\mathbf{p}}$ and the potential is averaged, we find:

$$\bar{R}_{20} = \frac{\mu C_{20}}{2a^3(1-e^2)^{3/2}} \left[5 - 3\left(\hat{\mathbf{h}} \cdot \hat{\mathbf{p}}\right)^2 \right] \tag{56}$$

where $\hat{\mathbf{h}}$ is the unit vector along the orbit normal.

Now we wish to specify this force potential in our frame of choice, where we assume that the rotation pole of the asteroid, $\hat{\mathbf{p}}$, is specified by its obliquity angle β and its right ascension α and $\hat{\mathbf{h}} = \sin i \sin \Omega \hat{\mathbf{x}} - \sin i \cos \Omega \hat{\mathbf{y}} + \cos i \hat{\mathbf{z}}$, so the general force potential in this frame becomes:

$$\bar{R}_{20} = \frac{\mu C_{20}}{2a^3(1-e^2)^{3/2}} \left[5 - 3\left(\sin \beta \sin i \cos(\alpha - \Omega) + \cos \beta \cos i\right)^2 \right] \tag{57}$$

Analysis of this potential shows that $\bar{R}_{20} = \text{constant}$, implying that $\hat{\mathbf{h}} \cdot \hat{\mathbf{p}}$ is constant which means that the orbit plane inclination relative to the rotation pole $\hat{\mathbf{p}}$ is a fixed quantity. Also derivable from this form of the equations is that the precession rate about the orbit pole is a constant equal to $3nC_{20}/2p^2 \hat{\mathbf{h}} \cdot \hat{\mathbf{p}}$ and that the argument of periapsis has a rate of advance equal to $3nC_{20}/4p^2 \left[1 - 5(\hat{\mathbf{h}} \cdot \hat{\mathbf{p}})^2 \right]$.

5 Stability of the Frozen Orbit Solutions

5.1 Stability of the Frozen Orbit

To study the stability of the frozen orbits defined above may seem to be a redundant exercise, given that the general solution of motion in these systems has been defined and is oscillatory. However, it is important to understand how these oscillations manifest themselves, especially when we consider the effect of joint perturbations between the SRP and mass distribution effects. For this stability analysis it is easier to work with the orbital elements themselves, as they do not have the non-linear constraints on magnitudes, etc., that the angular momentum and eccentricity vectors inherit.

We consider the two frozen orbit solutions in turn. In both cases we use the averaged force potential given in the form:

$$\bar{R}_g = -\frac{3aeg}{2}\hat{\mathbf{d}} \cdot \hat{\mathbf{e}} \tag{58}$$

$$\hat{\mathbf{e}} = [\cos\omega\cos\Omega - \sin\omega\sin\Omega\cos i]\,\hat{\mathbf{x}}$$
$$+ [\cos\omega\sin\Omega + \sin\omega\cos\Omega\cos i]\,\hat{\mathbf{y}} + \sin\omega\sin i\hat{\mathbf{z}} \tag{59}$$

and the vector $\hat{\mathbf{e}}$ is stated in our reference frame of choice where we align $\hat{\mathbf{d}} = \hat{\mathbf{x}}$. In the current discussion we do not shift to true anomaly as independent variable, as this will complicate the inclusion of the asteroid oblateness perturbation later.

As a first step we restate the Lagrange equations for this perturbing force function, noting that $\dot{a} = 0$:

$$\frac{de}{dt} = -\frac{3g}{2na}\sqrt{1-e^2}\left[\sin\omega\cos\Omega + \cos\omega\sin\Omega\cos i\right] \tag{60}$$

$$\frac{di}{dt} = -\frac{3g}{2na}\frac{e}{\sqrt{1-e^2}}\cos\omega\sin\Omega\sin i \tag{61}$$

$$\frac{d\omega}{dt} = -\frac{3g}{2na}\frac{1}{e\sqrt{1-e^2}}\left[(1-e^2)\cos\omega\cos\Omega - \sin\omega\sin\Omega\cos i\right] \tag{62}$$

$$\frac{d\Omega}{dt} = -\frac{3g}{2na}\frac{e}{\sqrt{1-e^2}}\sin\omega\sin\Omega - \dot{\nu} \tag{63}$$

$$\frac{d\sigma}{dt} = \frac{3g}{2na}\frac{1+e^2}{e}\left[\cos\omega\cos\Omega - \sin\omega\sin\Omega\cos i\right] \tag{64}$$

where we note that this is stated in a rotating reference frame, captured by including the angular rate, $\dot{\nu}$, of the asteroid about the sun.

Due to its applicability, we only consider the stability of the terminator plane frozen orbit solution: $i = \pi/2$, $\sin\Omega\sin\omega = -1$, and $e = \cos\Lambda$. Linearizing the Lagrange equations about this solution in terms of variables e, i, ω, and Ω yields:

$$\frac{d\delta e}{dt} = -\frac{3g}{2na}\sin\Lambda\delta\Omega \tag{65}$$

$$\frac{d\delta i}{dt} = -\frac{3g}{2na}\cot\Lambda\delta\omega \tag{66}$$

$$\frac{d\delta\omega}{dt} = \frac{3g}{2na}\frac{1}{\sin\Lambda\cos\Lambda}\delta i \tag{67}$$

$$\frac{d\delta\Omega}{dt} = \frac{3g}{2na}\frac{1}{\sin^3\Lambda}\delta e \tag{68}$$

Thus, the system splits into two uncoupled harmonic oscillators. If we express these in terms of eccentricity and inclination with true anomaly as the independent parameter we find:

$$\delta e'' = -\frac{1}{\cos^2\Lambda}\delta e \tag{69}$$

$$\delta i'' = -\frac{1}{\cos^2\Lambda}\delta i \tag{70}$$

with the oscillation period being $2\pi\cos\Lambda$, which is to be expected given the general solution found for motion in this system.

5.2 Perturbation from the Oblateness

Now we want to consider the effect of central body oblateness on these frozen orbits. A reasonable assumption is that if the orbit semi-major axis is large, the effect of the asteroid shape may be small and negligible. When the asteroid is small, however, the maximum semi-major axis becomes small and must lie close to the body, raising the possibility for a destabilizing interaction between the SRP and oblateness perturbations.

We will evaluate this interaction by assuming that the spacecraft lies in a frozen orbit and then include the secular rates from oblateness as a constant perturbation in the Lagrange equations. The resulting system can be solved to find the maximum oscillation amplitude in the orbit element of interest, in this case the eccentricity and inclination.

Our main interest is in the terminator frozen orbits, due to their favorable properties. Thus we will only study the effect of oblateness on this class of frozen orbit. To do so we must evaluate the rate of change of each of the orbit elements due to this perturbation at the frozen orbit conditions, stated previously. Doing so we find $\dot{a} = \dot{e} = 0$ and:

$$\frac{di}{dt} = \frac{3}{4}\frac{n(I_a - I_t)}{a^2 \sin^4 \Lambda} \sin^2 \beta \sin 2\alpha \tag{71}$$

$$\frac{d\omega}{dt} = \frac{3}{4}\frac{n(I_a - I_t)}{a^2 \sin^4 \Lambda} \left[5 - 3\sin^2 \beta \sin^2 \alpha\right] \tag{72}$$

$$\frac{d\Omega}{dt} = (\pm)_\Omega \frac{3}{4}\frac{n(I_a - I_t)}{a^2 \sin^4 \Lambda} \sin 2\beta \sin \alpha \tag{73}$$

$$(\pm)_\Omega = \sin \Omega \tag{74}$$

We can insert these nominally constant terms on the right-hand side of Eqns. 65 - 68 to form a set of non-homogenous equations. Given the simple form of the linearized solutions, the general solution for these terms can be found assuming an initial orbit evaluated at the frozen orbit conditions.

$$\begin{bmatrix} \delta i \\ \delta \omega \end{bmatrix} = \frac{3}{4}\frac{n(I_a - I_t)}{a^2 \sin^4 \Lambda}\frac{1}{\dot{\nu}} \tag{75}$$

$$\begin{bmatrix} \cos \Lambda \left\{ \sin^2 \beta \sin^2 \alpha \left[\sin(\nu/\cos \Lambda) + 3\cos \Lambda (1 - \cos(\nu/\cos \Lambda))\right] \\ -5\cos \Lambda (1 - \cos(\nu/\cos \Lambda))\right\} \\ \\ \sin^2 \beta \sin^2 \alpha \left[(1 - \cos(\nu/\cos \Lambda)) + 3\cos \Lambda \sin(\nu/\cos \Lambda)\right] \\ +5\cos \Lambda \sin(\nu/\cos \Lambda) \end{bmatrix}$$

and

$$\begin{bmatrix} \delta e \\ \delta \Omega \end{bmatrix} = (\pm)_\Omega \frac{3}{4}\frac{n(I_a - I_t)}{a^2 \sin^4 \Lambda}\frac{\sin 2\beta \sin \alpha}{\dot{\nu}}$$

$$\begin{bmatrix} -\cos^2 \Lambda (1 - \cos(\nu/\cos \Lambda)) \\ \cos \Lambda \sin(\nu/\cos \Lambda) \end{bmatrix} \tag{76}$$

These results can be used to evaluate the fluctuation amplitude in these orbit elements from their nominal values, especially in eccentricity, in order to determine if the variation is acceptable. If the amplitude becomes too large the linearization assumption we have made will be violated, and a full non-linear evaluation should be made. We note that the amplitude of oscillation will change as the asteroid moves about the sun. The variation in eccentricity from its nominal value, $\cos \Lambda$, is bounded by:

$$|\delta e| < \frac{3}{2}\frac{n(I_a - I_t)}{a^2}\frac{\cos^2 \Lambda}{\sin^4 \Lambda}\frac{\sin 2\beta \sin \alpha}{\sqrt{\mu_{sun}P}}d^2 \tag{77}$$

The deviation in e will decrease with an increasing semi-major axis, however there also exists an upper bound on a for the spacecraft to remain trapped. To determine the minimum deviation in eccentricity due to the asteroid's oblateness, substitute the value $a_{max} = \sqrt{3\mu/g}/4$ into the above to find:

$$|\delta e|_{min} = \left(\frac{16}{3}\right)^2 \frac{(I_a - I_t)}{\mu}\frac{\cos \Lambda}{\sin^3 \Lambda} \sin 2\beta \sin \alpha \frac{\beta}{d^2} \tag{78}$$

where for this formula the assumption is that the orbit is adjusted to always be at the maximum distance. Thus, the second formula has the smallest perturbation at aphelion while Eqn. 77, for a fixed semi-major axis, has the maximum perturbation at aphelion.

5.3 Perturbation from Ellipticity

For the ellipticity effect, we rely on the numerical analysis given in [5] where it is empirically determined that orbits outside of 1.5 resonance radii are not subject to destabiliziation due to the orbit ellipticity. The resonance radius is the orbit semi-major axis where the orbit period equals the rotation period and equals $\left(\mu T^2/(4\pi^2)\right)^{1/3}$. Thus, for rapidly rotating bodies one can in principle orbit more closely, while for slowly rotating bodies one must in general maintain a greater distance. The 1.5 resonance radius limit we state does not make any assumption about the orientation of the rotation pole, and is only sharp if the orbit inclination is less than 45 degrees in general. For high inclination orbits, especially for retrograde orbits with inclinations greater than 135 degrees, it becomes possible to orbit much more closely to the body without suffering any effects from the ellipticity. In these situations, however, the oblateness becomes a major perturbation. Thus, the orbit limit to guard against ellipticity effects can be stated as:

$$a \quad > \quad \frac{3}{2}\left(\frac{T^2\mu}{4\pi^2}\right)^{1/3} \tag{79}$$

where T is the rotation period of the asteroid. In general, once the orbit pole of the asteroid is known it is possible to immediately map out when the terminator orbits will have to take special care relative to their interaction with the asteroid gravity field distribution.

5.4 Destabiliziation Mechanism

The mechanism for destabilization can include two different effects. First is the the oblateness alone, which may induce large oscillations in the frozen orbit elements which then excite the longer-term oscillations in the orbit elements which can lead to growth in the eccentricity. This form is not as serious, as it generally takes longer for the instability to become pronounced, and even then it follows a well defined solution. More difficult to deal with is the joint action of the oblateness and the ellipticity. Here, variations in the eccentricity can cause the orbit periapsis to drop, given that a is constant on average. If the amplitude becomes large enough, and the alignment of the orbit pole with the rotation pole is direct, resonant interactions between the spacecraft orbit and the asteroid rotation rate can cause changes in the orbit semi-major axis, eccentricity, and inclination. Variations in any of these can become reinforced, causing larger oscillations which send periapsis closer to the asteroid which further destabilizes the motion. When designing an orbit, this is the main mechanism to avoid, captured by the 1.5 resonance radius condition above, as this can destabilize an orbit rapidly.

6 Example Computations

In the following we provide some example computations for orbit mechanics of a spacecraft about two different asteroids, one relatively small and the other a bit larger. The spacecraft model we choose has a mass to area ratio of 33 kg/m^2, corresponding to a projected area (including solar arrays) of 12 m^2 and a mass of $\sim$ 400 kg. For simplicity we chose a reflectance $\rho = 0$. We modeled the motion of the spacecraft about two different asteroids modeled after NEA candidates for a mission. We call these Asteroid I and Asteroid II.

Asteroid I has semi-major axes of $214 \times 100 \times 100$ meters, an assumed density of 2 g/cm^3, an assumed rotation period of 12 hours, and an assumed obliquity of 45°. It's heliocentric orbit has a perihelion of 1.03 AU and an aphelion of 2.7 AU.

Asteroid II is larger and has semi-major axes of $635 \times 317 \times 317$ meters, an assumed density of 2 g/cm^3, an assumed rotation period of 19 hours, and an assumed obliquity of 45°. It's heliocentric orbit has a perihelion of 1.1 AU and an aphelion of 1.45 AU.
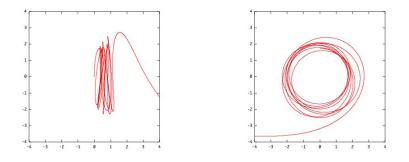
Figure 1: Examples of an escaping orbit due to solar radiation pressure perturbations for Asteroid I. The left image is the trajectory as viewed from the sun, the right is as viewed in the terminator plane with the sun to the left. The spacecraft escapes when the asteroid approaches perihelion and a_{max} is violated.
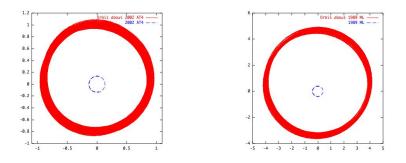

Figure 2: Long-term stable orbits about Asteroid I (left) and Asteroid II (right). These orbits are viewed from the Sun to the asteroid and both are propagated for over a year, through the asteroid perihelion passage.

7   Conclusions

Spacecraft orbiting about small solar system bodies such as asteroids and comets must contend with significant perturbations from solar radiation pressure, the body mass distribution, and solar gravitation. Orbit mechanics in the presence of each of these perturbations can be analyzed in detail, and in some special cases joint perturbation effects can be added. This paper states the known orbit mechanics results for motion in the presence of these perturbations and analyzes the effect of joint perturbations on the orbital motion of a spacecraft.
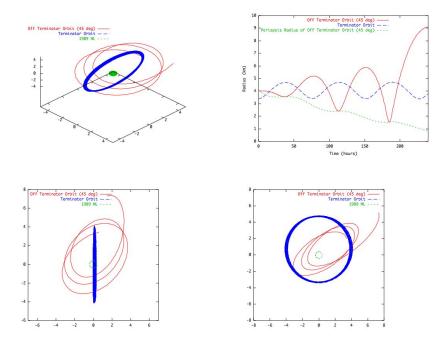
Figure 3: Two orbits about Asteroid II, one chosen in the terminator plane according to the nominal frozen orbit design and the other started 45 degrees out of the terminator plane in a circular orbit. The non-nominal design impacts on the asteroid in a little over 10 days.
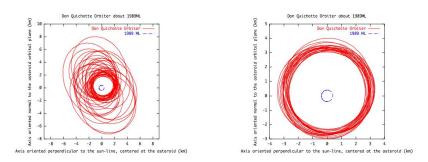

Figure 4: Example orbits about Asteroid II. Left, initial orbit radius of 2 km, at a distance where resonance effects from the mass distribution are important. Right, initial orbit radius of 3 km, outside the reach of the mass distribution effects.

References

[1] Kawaguchi, J. "Hayabusa, Summary of Guidance, Navigation and Control Achievement in its Proximity Phase," paper presented at the 2006 AIAA/AAS Astrodynamics Specialist Meeting, Keystone, Colorado, August 2006. Paper AIAA-2006-6533.

[2] D.J. Scheeres. 1994. Dynamics About Uniformly Rotating Tri-Axial Ellipsoids. Applications to Asteroids, Icarus 110:22538.

[3] D.J. Scheeres, S.J. Ostro, R.S. Hudson, and R.A. Werner. 1996. Orbits Close to Asteroid 4769 Castalia, Icarus 121:6787.

[4] D.J. Scheeres, B.G. Williams, and J.K. Miller. 2000. Evaluation of the Dynamic Environment of an Asteroid: Applications to 433 Eros, Journal of Guidance, Control and Dynamics 23:466475.

[5] Hu, W. and Scheeres, D.J. Numerical Determination of Stability Regions for Orbital Motion in Uniformly Rotating Second Degree and Order Gravity Fields. Planetary and Space Science 52: 685-692, 2004.

[6] Scheeres, D.J. Satellite Dynamics about Small Bodies: Averaged Solar Radiation Pressure Effects. Journal of the Astronautical Sciences 47(1): 25-46, 1999.

[7] Scheeres, D.J. and Marzari, F. Spacecraft Dynamics in the Vicinity of a Comet. Journal of the Astronautical Sciences 50(1): 35-52, 2002.

[8] Morrow, E., Scheeres, D.J., and Lubin, D. Solar Sail Orbit Operations at Asteroids. Journal of Spacecraft and Rockets 38(2): 279286, 2001.

[9] D.J. Scheeres, R. Gaskell, S. Abe, O. Barnouin-Jha, T. Hashimoto, J. Kawaguchi, T. Kubota, J. Saito, M. Yoshikawa, N. Hirata, T. Mukai, M. Ishiguro, T. Kominato, K. Shirakawa, M. Uo. The Actual Dynamical Environment About Itokawa, paper presented at the 2006 AIAA/AAS Astrodynamics Specialist Meeting, Keystone, Colorado, August 2006. Paper AIAA-2006-6661

[10] D. Boccaletti and G. Pocacco. Theory of Orbits, Springer, 1996.

[11] H. Dankowicz. "Some special orbits in the two-body problem with radiation pressure," *Celestial Mechanics and Dynamical Astronomy* 58: 353-370, 1994.

[12] H. Dankowicz. "The two-body problem with radiation pressure in a rotating reference frame," *Celestial Mechanics and Dynamical Astronomy* 61: 287-313, 1995.

[13] H. Dankowicz. "Escape of particles orbiting asteroids in the presence of radiation pressure through separatrix splitting," *Celestial Mechanics and Dynamical Astronomy* 67: 63-85, 1997.

[14] H. Dankowicz. "Slow diffusion and effective stability of dust particles orbiting asteroids," *Celestial Mechanics and Dynamical Astronomy* 84: 1-25, 2002.

[15] F. Mignard and M. Hénon. "About an unsuspected integrable problem," *Celestial Mechanics and Dynamical Astronomy* 33: 239-250, 1984.

[16] K. Richter and H.U. Keller. "On the stability of dust particle orbits around cometary nuclei," *Icarus* 114: 355-371, 1995.

[17] D.J. Scheeres, S.J. Ostro, R.S. Hudson, E.M. DeJong, and S. Suzuki. "Orbit dynamics about 4179 Toutatis," *Icarus* 132:53–79, 1998.